Broadcasting of quantum correlations in qubit-qudit systems

Rounak Mundra,[1] Dhrumil Patel,[1] Indranil Chakrabarty,[2,3] Nirman Ganguly,[4] and Sourav Chatterjee[1,3,5,6,*]

[1]*Center for Computational Natural Sciences and Bioinformatics, International Institute of Information Technology-Hyderabad, Gachibowli, Telangana-500032, India*

[2]*Center for Security, Theory and Algorithmic Research, International Institute of Information Technology-Hyderabad, Gachibowli, Telangana-500032, India*

[3]*Harish-Chandra Research Institute, HBNI, Chhatnag Road, Jhunsi, Uttar Pradesh 211019, India*

[4]*Department of Mathematics, Birla Institute of Technology and Science Pilani, Hyderabad Campus, Telangana-500078, India*

[5]*SAOT, Erlangen Graduate School in Advanced Optical Technologies, Paul-Gordan-Strasse 6, D-91052 Erlangen, Germany*

[6]*Raman Research Institute, Sadashivanagar, Bangalore, Karnataka-560080, India*

(Received 3 May 2019; published 18 October 2019)

Quantum mechanical properties like entanglement, discord, and coherence act as fundamental resources in various quantum information processing tasks. Consequently, the technique of generating more resources from a few, typically termed as broadcasting, serves as a promising candidate for the design of quantum networks. One way to broadcast resources could be using a cloning operation. In this article, broadcasting of quantum resources beyond $2 \otimes 2$ systems is investigated. In particular, in $2 \otimes 3$ dimensions, a class of states not useful for broadcasting of entanglement is characterized considering an optimal universal Heisenberg cloning machine. The broadcasting ranges for maximally entangled mixed states and two-parameter class of states are obtained to exemplify our protocol. A significant derivative of our protocol is that the cloning operation generates a qutrit $(3 \otimes 3)$ entangled pair with positive partial transpose on one of the local sides, and an absolutely separable qubit $(2 \otimes 2)$ pair on the other side of the input bipartite $2 \otimes 3$-dimensional resource state. Moving beyond entanglement, in $2 \otimes d$ dimensions, the impossibility to optimally broadcast quantum discord and quantum coherence (l_1 norm) is established. However, some significant illustrations are provided to highlight that nonoptimal broadcasting of discord and coherence is still possible.

DOI: 10.1103/PhysRevA.100.042319

I. INTRODUCTION

Quantum entanglement [1] acts as an invaluable resource in most information processing tasks [2–8]. It cannot be increased by local operations and classical communication (LOCC). However, nonlocal unitary operations on the composite system can generate entanglement between separable states, a fact used in experimental generation of entangled states [9]. However, there are *absolutely separable states* which preserve their separability under any nonlocal unitary action. Their characterization is an important problem in quantum computing, especially in the context of NMR-based quantum computing [10]. Another important feature in entanglement theory is the existence of entangled states with positive partial transpose (PPT) [11,12]. Though these PPT entangled states (PPTES) aren't commonly useful for information processing tasks, they aid in some cryptographic protocols [13].

A quantum network with entangled nodes can perform quantum information processing tasks by creating, distributing, and processing quantum information [14]. Precise routing of entanglement along with controlled manipulation of remote quantum entanglement through the nodes of a quantum network would be a major stepping stone towards a quantum internet [14–16] including various other applications such as distributed quantum computing [17], precision sensing [18], and blind quantum computing (i.e., computing on encrypted data) [19]. In such a quantum network, there can always be an exigency in increasing the number of available entangled pairs across the various nodes. One way to accomplish the task, primarily termed as "broadcasting of entanglement," is via the application of local [20,21] and nonlocal (global) [21,22] copying operations. Although perfect cloning [23] as well as perfect broadcasting of correlation [24] of an arbitrary quantum state is impossible, approximate versions of both cloning [25,26] and broadcasting [20–22] operations on an arbitrary quantum state has been successfully achieved. In the technique of "broadcasting of entanglement," two parties namely Alice and Bob, either use local cloners on their individual subsystems or nonlocal cloner jointly on the entire (combined) system to create two output pairs which remain entangled over a finite range of input state parameters. More particularly, in Ref. [27], researchers showed that universal quantum cloning machines (UQCMs) [25] having fidelity above $\frac{1}{2}(1 + \frac{1}{\sqrt{3}})$ can broadcast entanglement via local cloning operations. There they also proved that entanglement in the input state is optimally broadcast only if the quantum cloner used for local coping is optimal [28]. Later, it was shown that optimal broadcasting of entanglement is only possible when symmetric cloners are used [29,30]. Recent

*Present affiliation: Raman Research Institute, Sadashivanagar, Bangalore, Karnataka-560080, India.

works on broadcasting of entanglement were done by using symmetric [21] and asymmetric cloners [30], considering two-qubit general bipartite states as the input resource.

Quantum discord [31,32] is a type of quantum correlation which extends beyond the idea of entanglement. Besides supplementing the measure of entanglement defined on the system of interest, discord can also act as a resource [33]. Similar to broadcasting of entanglement, broadcasting of quantum correlations beyond entanglement (discord) has been explored in two-qubit systems [21,30]. The motivation to study the broadcasting of such correlations is not only for their use in qutrits and higher qudits in quantum information theory, but also for the study of spins chains with spin values larger than $\frac{1}{2}$ [34,35].

Just like entanglement and discord, quantum coherence is also a critical resource [36] for many information processing tasks. It outlines the departure of the classical from the quantum world and is often considered as a measure of superposition of quantum states [37]. Quantum coherence has been used for crucial processes like better cooling [38,39], or for work extraction in nanoscale thermodynamics. Coherence has also played a part in quantum algorithms [40–42], in biological processes [43], and in establishing a general wave-particle duality relation [44–46]. Owing to the significant utility of these resources in quantum information processing, in literature, researchers have successfully demonstrated the generation of more pairs with lesser degree of coherence given a highly coherent pair using the technique of broadcasting via cloning operation [47]. It is important to clarify here that the coherence we are referring to belongs to the general superposition of basis states with respect to the choice of orthonormal bases [37]. In literature, this is referred to as *speakable coherence* [48] and considering it, many resource theories have been formulated [36,49]. However, there also exists another notion of coherence defined from perspective of quantum thermodynamics called *unspeakable coherence* [48]. This coherence takes into account the superposition of energy eigenstates of a given Hamiltonian. Unlike *speakable coherence*, the allowed set of transformations for *unspeakable coherence* are limited to only covariant operations [48]. It was shown in [50] that this later kind of coherence cannot be broadcast.

Broadcasting of entanglement still remains an unexplored topic in higher dimensional systems. Such a question gains practical importance as higher dimensional entanglement provides a larger information processing capability than the conventional two-dimensional (qubit) entangled pairs [51]. It also plays a major role in quantum communication [52,53], quantum computation [54,55], and quantum cryptography [56,57] tasks where mere qubit entanglement is not enough. This increase in quantum information processing capability with the availability of higher dimensional quantum resources is not confined to entanglement but also, in general, extends to discord and coherence. To investigate this unexplored direction, in this article, we increase the dimension on one of the partitions of our input bipartite resource to an arbitrary value "$d > 2$". As a first step, we study the broadcasting of entanglement and then for other resources (like discord and coherence) in such qubit-qudit ($2 \otimes d$) systems with symmetric cloning operations. Here, it is crucial to mention that our results are consistent with the previous studies in lower dimensions and for the $d = 2$ case, they reduce to those in [21,22,27,47]. In order to prohibit the violation of the "no-broadcasting theorem" [24] and the "monogamy of entanglement" [58], we constrain our methods to achieve approximate broadcasting of correlations via cloning.

In the present contribution, we study the problem of broadcasting of quantum resources (i.e., entanglement, discord, and coherence) in $2 \otimes 3$ (qubit-qutrit) and, more generally, in $2 \otimes d$ (qubit-qudit)-dimensional systems. This article is structured as follows. In Sec. II, we give a brief description of the related concepts which have been used to derive the results in the subsequent sections of this article. In Sec. III, we study broadcasting of entanglement considering the most general class of state in $2 \otimes 3$ dimensions as the input resource and we provide the nonbroadcastable ranges for it. We further exemplify our study by considering maximally entangled mixed states (MEMS) and two parameter class of states (TPCS) individually as our input resources. For each of these example classes, we also characterize the broadcastable zones. As an important derivative of our protocol, in $2 \otimes 3$ dimensions, we observe that the cloned qubit pair on Alice's local side is an absolutely separable state, while the cloned qutrit pair on Bob's local side belongs to the PPTES class. In Sec. IV, we provide rigorous proofs to claim the impossibility of optimal broadcasting of discord and coherence in general qubit-qudit systems. Thereafter we consider few examples and corresponding graphical illustrations to show that nonoptimal broadcasting of these resources is, however, possible. These findings help us to generalize the impossibilities derived in [21,47]. Finally, we provide the concluding remarks in Sec. V. A summary of the previous contributions in this direction, in contrast to those in this work is explicitly presented in Table I.

II. USEFUL DEFINITIONS AND CONCEPTS

In this section, we give a brief introduction to various concepts which will be useful and related to the main theme of the article.

A. General qubit-qudit mixed state

In this article, we have considered a general qubit-qudit mixed state as a resource state which is represented in the canonical form as

$$\rho = \frac{1}{2d}\left(\mathbb{I}_2 \otimes \mathbb{I}_d + \sum_{i=1}^{3} x_i \sigma_i \otimes \mathbb{I}_d + \sum_{j=1}^{d^2-1} y_j \mathbb{I}_2 \otimes O_j + \sum_{i=1}^{3}\sum_{j=1}^{d^2-1} T_{ij}\sigma_i \otimes O_j\right). \tag{1}$$

Here $x_i = \mathrm{Tr}[\rho(\sigma_i \otimes \mathbb{I}_d)]$, $y_j = \mathrm{Tr}[\rho(\mathbb{I}_2 \otimes O_j)]$, $T_{ij} = \mathrm{Tr}[\rho(\sigma_i \otimes O_j)]$, σ_i's are 2×2 Pauli matrices, and O_j's are $(d^2 - 1)$ linearly independent operators defining an operator basis for the d-dimensional subsystem with an additional property $\mathrm{Tr}(O_i O_j) = \delta_{ij}$. Here, $\mathbb{I}_d$ is the identity matrix of order d. Tr is the trace operation on a given matrix and δ_{ij} is the Kronecker delta symbol.

TABLE I. Summary of earlier results along with those in the present work on broadcasting of entanglement, discord, and coherence. The abbreviations such as NME, MEMS, TPCS, two-qubit general, qubit-qutrit general, and qubit-qudit general stand for nonmaximally entangled state, maximally entangled mixed state, two-parameter class of states, general two-qubit mixed state, general qubit-qutrit mixed state, and general qubit-qudit mixed state classes, respectively.

System's dimension	Resource state	Broadcasting of	Cloning operation	Author(s)
$2 \otimes 2$	NME	Entanglement	Symmetric	Buzek *et al.* and Hillery [20,22]
$2 \otimes 2$	NME	Entanglement	Symmetric	Bandyopadhyay *et al.* [27]
$2 \otimes 2$	NME	Entanglement	Asymmetric	Ghiu [29]
$2 \otimes 2$	Two-qubit general	Entanglement and discord	Symmetric	Chatterjee *et al.* [21]
$2 \otimes 2$	Two-qubit general	Entanglement and discord	Asymmetric	Jain *et al.* [30]
$2 \otimes 2$	Two-qubit general	Coherence	Symmetric	Sharma *et al.* [47]
$2 \otimes 3$	Qubit-qutrit general	Entanglement	Symmetric	This work
$2 \otimes 3$	MEMS and TPCS	Entanglement	Symmetric	This work
$2 \otimes d$	Qubit-qudit general	Discord	Symmetric	This work
$2 \otimes d$	Qubit-qudit general	Coherence	Symmetric	This work

As an example, a general qubit-qutrit mixed entangled state ρ_{12} is given by

$$\rho_{12} = \frac{1}{6}\Bigg(\mathbb{I}_6 + \sum_{i=1}^{3} x_i \sigma_i \otimes \mathbb{I}_3 + \sum_{i=1}^{8} y_i \mathbb{I}_2 \otimes G_i + \sum_{i=1}^{3}\sum_{j=1}^{8} T_{ij}\sigma_i \otimes G_j\Bigg) = \{\vec{X}, \vec{Y}, T\}, \tag{2}$$

where $x_i = \mathrm{Tr}[\rho_{12}(\sigma_i \otimes \mathbb{I}_3)]$, $y_i = \mathrm{Tr}[\rho_{12}(\mathbb{I}_2 \otimes G_i)]$, $T_{ij} = \mathrm{Tr}[\rho_{12}(\sigma_i \otimes G_j)]$, σ_i's are Pauli matrices, and G_j's are Gell-Mann matrices. $\vec{X}$, $\vec{Y}$, and T are the Bloch vectors and the correlation matrix, respectively.

B. Detection of entanglement

In order to test the separability of a given bipartite state, we generally use the Peres-Horodecki (PH) criterion [59]. This criterion is a necessary and sufficient condition for detection of entanglement for bipartite systems with dimensions $2 \otimes 2$ and $2 \otimes 3$.

1. Peres-Horodecki criterion

If at least one of the eigenvalues of a partially transposed density operator for a bipartite state ρ defined as $\rho^{T}_{m\mu,\eta\nu} = \rho_{mv,\eta\mu}$ turns out to be negative, then we can say that the state ρ is entangled. Equivalently, this criterion can be translated to the condition that the determinant of at least one of the two matrix,

$$W_3 = \left(\begin{array}{cc|c} \multicolumn{2}{c|}{W_2} & \begin{matrix}\rho_{00,10}\\ \rho_{00,11}\end{matrix} \\ \hline \rho_{10,00} & \rho_{11,00} & \rho_{10,10} \end{array}\right) \text{ or}$$

$$W_4 = \left(\begin{array}{ccc|c} \multicolumn{3}{c|}{W_3} & \begin{matrix}\rho_{01,10}\\ \rho_{01,11}\\ \rho_{11,10}\end{matrix} \\ \hline \rho_{10,01} & \rho_{11,01} & \rho_{10,11} & \rho_{11,11} \end{array}\right), \tag{3}$$

is negative; with determinant of $W_2 = \left[\begin{smallmatrix}\rho_{00,00} & \rho_{01,00}\\ \rho_{00,01} & \rho_{01,01}\end{smallmatrix}\right]$ being simultaneously non-negative.

As PH criterion requires us to compute eigenvalues, it is not always computationally feasible to compute eigenvalues of the density matrix that have several variables as an argument. To overcome this problem, we have used another separability criterion in terms of Bloch parameters $(\vec{X}, \vec{Y}, T)$ which is comparatively easier to compute.

2. Separability criterion in terms of Bloch parameters

In order to check separability, we have used the separability criterion [60] in terms of Bloch sphere representation of two quantum mechanical systems. This criterion makes use of the Ky Fan matrix norm. Let A be a matrix that belongs to $\mathbb{C}^{m\times n}$. The Ky Fan matrix norm is defined as the sum of singular values χ_i,

$$||A||_{\mathrm{KF}} = \sum_{i=1}^{\min\{m,n\}} \chi_i = \mathrm{Tr}\sqrt{A^{\dagger}A}. \tag{4}$$

This criterion states that if a bipartite state of $M \otimes N$ satisfies

$$\sqrt{\frac{2(M-1)}{M}}||X||_2 + \sqrt{\frac{2(N-1)}{N}}||Y||_2 + \sqrt{\frac{4(M-1)(N-1)}{(MN)}}||T||_{KF} \leqslant 1, \tag{5}$$

then it is a separable state. Here $||.||_2$ is the Euclidean norm.

Therefore if a bipartite state of $2 \otimes 3$ dimensions with Bloch representation (2) satisfies

$$||X||_2 + \sqrt{\frac{4}{3}}||Y||_2 + \sqrt{\frac{4}{3}}||T||_{KF} \leqslant 1, \tag{6}$$

then it is a separable state. However, if the state violates this condition, we cannot conclude whether the state is separable or entangled.

C. Absolutely separable states

In the resource theory of entanglement, local operations and classical communication are considered to be free operations, as entanglement does not increase under LOCC. Local unitaries are subsets of LOCC, and under their action, entanglement remains unchanged. However, nonlocal or global

unitary operations are not free as they can turn a separable state into an entangled state. The CNOT operation is one of the fundamental global unitary operations which can change even a product state to an entangled state.

However, there are separable states which can preserve separability under any arbitrary global unitary operation. These states are termed as absolutely separable states [61]. If we denote the set of separable states by **S** and absolutely separable states by **AS**, then $\mathbf{AS} = \{\chi : U\chi U^\dagger \in \mathbf{S} \ \forall \ U\}$. Here U denotes an unitary operator. It has been proven in [62] that a two-qubit state is absolutely separable iff $\lambda_1 \leqslant \lambda_3 + 2\sqrt{\lambda_2\lambda_4}$, where λ_i's are the eigenvalues of the density matrix of the state arranged in descending order. Later on in [63], the condition was extended to states in $2 \otimes d$ dimensions. Another interesting feature of the absolutely separable states is that they form a convex and compact set within the set of separable states [64].

D. PPT entangled states

Pure entangled states can be distilled from a large number of mixed entangled states for use in quantum information protocols. However, there are mixed entangled states from which no pure entangled state can be extracted. Subsequently, they came to be known as bound entangled states [11].

It was noted that any entangled state which has a positive partial transpose is bound entangled (also known as undistillable) and literature is rich with examples of entangled states having positive partial transpose [12]. However, the question whether a state which has a negative partial transpose (NPT) is bound entangled is still open.

Although a weaker form of entanglement, PPTES have found utility in information protocols like quantum key generation [13]. Therefore, both from a mathematical and physical perspective, generation of PPTES is an intriguing problem in quantum information science. Most of the constructions of PPTES have been through mathematical rigor, the number of physical constructions being rare.

The *realignment criterion* is one of the simplest tests that can detect entanglement in PPT states. It states that all separable states $\rho \in M_m \otimes M_n$ satisfy $||R(\rho)||_{tr} \leqslant 1$, where R: $M_m \otimes M_n \to M_{m,n} \otimes M_{m,n}$ is the linear "realignment" map defined on elementary tensors by $R(|i\rangle\langle j| \otimes |k\rangle\langle l|) = |i\rangle\langle k| \otimes |j\rangle\langle l|$. $||R(\rho)||_{tr} > 1$, is a signature of the entanglement of ρ.

E. Cloning

As stated previously, the no-cloning theorem states that given an arbitrary quantum state $|\psi\rangle$, there doesn't exist any completely positive trace preserving map (CPTP) C that can transform a single copy of $|\psi\rangle$ to two copies of $|\psi\rangle$, i.e., $C : |\psi\rangle \not\to |\psi\rangle \otimes |\psi\rangle$.

In our work, we are interested in symmetric $1 \to 1 + 1$ cloning machines. We use the symmetric version of the optimal universal asymmetric Heisenberg cloning machine. This machine creates the second clone with maximal fidelity for a given fidelity of the first one. The general unitary transformation for cloning of qudit by this machine is given by

$$\begin{aligned} &U|j\rangle_a|00\rangle_{bc} \\ &\to \sqrt{\frac{2}{d+1}}\Bigg(|j\rangle_a|j\rangle_b|j\rangle_c + \frac{1}{2}\sum_{r=1}^{d-1}|j\rangle_a|\overline{j+r}\rangle_b|\overline{j+r}\rangle_c \\ &\quad + \frac{1}{2}\sum_{r=1}^{d-1}|\overline{j+r}\rangle_a|j\rangle_b|\overline{j+r}\rangle_c\Bigg). \end{aligned} \tag{7}$$

Here, suffixes "a" and "b" represent clones, "c" represents the ancillary state, and "d" denotes the dimension.

F. Broadcasting of quantum resources by cloning

In this subsection, we give a brief exposure to the idea of broadcasting of resources with the help of cloning machines. It is known that entanglement, discord, and coherence can be used as a resource for a wide range of information processing tasks. Given that, there is always a necessity of creating a greater number of resource pairs with lesser resourcefulness from a single resource pair with a higher degree of resourcefulness. The process of decomposing a resource pair to a greater number of resource pairs is called broadcasting of quantum resources. We apply different strategies to do broadcasting of resources. One such strategy is to apply local cloning operations on each party subsystem sharing the resource. In the subsequent subsections, we describe how the broadcasting happens in qubit-qudit systems.

1. Broadcasting of entanglement

Let us consider that Alice and Bob share a general qubit-qudit mixed quantum state ρ_{12} (1) as an input state. Also, qubit 3 and qudit 4 serve as the initial blank state in Alice's and Bob's individual subsystem, respectively. We apply local cloning unitaries $U_a \otimes U_b$ (7) on qubits (1,3) and qudits (2,4). Tracing out the ancilla qubit and ancilla qudit on Alice's and Bob's side, respectively, we get the output state as $\tilde{\rho}_{1234}$. We trace out the $(2, 4)$ and $(1, 3)$ subsystems to obtain the local output states $\tilde{\rho}_{13}$ on Alice's side and $\tilde{\rho}_{24}$ on Bob's side, respectively. Similarly, after tracing out appropriate qubits and qudits from the output state, we obtain the two plausible groups of nonlocal output states $\tilde{\rho}_{14}$ and $\tilde{\rho}_{23}$. The process is illustrated in Fig. 1.

The expression for nonlocal outputs states across the subsystems of Alice and Bob are given by

$$\begin{aligned} \tilde{\rho}_{14} &= \mathrm{Tr}_{23}[\tilde{\rho}_{1234}] \\ &= \mathrm{Tr}_{23}[U_a \otimes U_b(\rho_{12} \otimes B_{34} \otimes M_{56})U_a^\dagger \otimes U_b^\dagger], \\ \tilde{\rho}_{23} &= \mathrm{Tr}_{14}[\tilde{\rho}_{1234}] \\ &= \mathrm{Tr}_{14}[U_a \otimes U_b(\rho_{12} \otimes B_{34} \otimes M_{56})U_a^\dagger \otimes U_b^\dagger], \end{aligned} \tag{8}$$

while the expression for local output states within Alice's and Bob's individual subsystem are given by

$$\begin{aligned} \tilde{\rho}_{13} &= \mathrm{Tr}_{24}[\tilde{\rho}_{1234}] \\ &= \mathrm{Tr}_{24}[U_a \otimes U_b(\rho_{12} \otimes B_{34} \otimes M_{56})U_a^\dagger \otimes U_b^\dagger], \\ \tilde{\rho}_{24} &= \mathrm{Tr}_{13}[\tilde{\rho}_{1234}] \\ &= \mathrm{Tr}_{13}[U_a \otimes U_b(\rho_{12} \otimes B_{34} \otimes M_{56})U_a^\dagger \otimes U_b^\dagger]. \end{aligned} \tag{9}$$

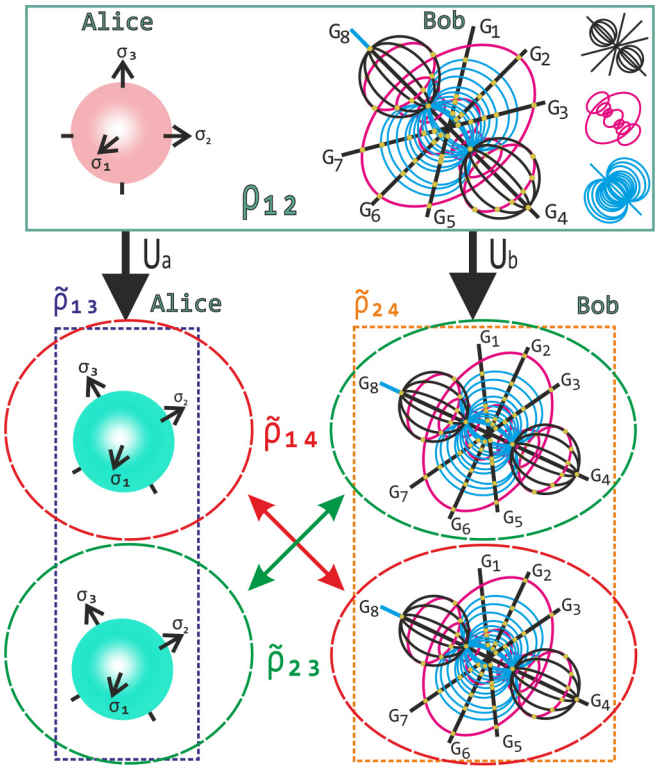

FIG. 1. A schematic depicting the application of local cloning unitaries U_a and U_b on a qubit-qutrit state shared between Alice and Bob. The qutrit system ($d = 3$) on Bob's side is illustrated with a three-sphere or glome [65] structure in the four-dimensional Euclidean space. Stereographic projection of the hypersphere's parallels (magenta), meridians (cyan), and hypermeridians (black) are illustrated separately, as subfigures on the right column, beside the glome qutrit for clarity. The projection being conformal, the circular curves intersect each other orthogonally at the yellow points. The rectangular box with a solid olive green boundary represents the input state ρ_{12}; the dotted rectangular envelopes in blue and orange highlight the cloned local output pairs $\tilde{\rho}_{13}$ and $\tilde{\rho}_{24}$, respectively. Further, the dotted oval-shaped envelopes in red and green depict the cloned nonlocal output pairs $\tilde{\rho}_{14}$ and $\tilde{\rho}_{23}$, respectively.

Here $B_{34} = |00\rangle\langle 00|$ and $M_{56} = |00\rangle\langle 00|$ represent the initial blank state and machine state, respectively.

The requirement is to broadcast entanglement between the desired pairs (1,4) and (2,3); we need to maximize the entanglement between nonlocal pairs (1,4) and (2,3) irrespective of the local pairs (1,3) and (2,4). However, for optimal broadcasting, we should ideally have no entanglement between local pairs, thereby increasing the amount of entanglement between nonlocal pairs.

Nonoptimal broadcasting of entanglement. An entangled state ρ_{12} is said to be broadcast after the application of local cloning operation $(U_a \otimes U_b)$, if the nonlocal output states $\{\tilde{\rho}_{14},\ \tilde{\rho}_{23}\}$ are inseparable for some input state parameters.

Optimal broadcasting of entanglement. An entangled state ρ_{12} is said to be broadcast optimally after the application of local cloning operation $(U_a \otimes U_b)$, if the nonlocal output states $\{\tilde{\rho}_{14},\ \tilde{\rho}_{23}\}$ are inseparable and the local output states $\{\tilde{\rho}_{13},\ \tilde{\rho}_{24}\}$ are separable for some input state parameters.

Suboptimal broadcasting of entanglement. An entangled state ρ_{12} is said to be broadcast suboptimally after the application of local cloning operation $(U_a \otimes U_b)$ for some input state parameters if the following conditions simultaneously hold.

(1) The nonlocal output states $\{\tilde{\rho}_{14},\ \tilde{\rho}_{23}\}$ are inseparable.

(2) Only one of the local output states $\{\tilde{\rho}_{13},\ \tilde{\rho}_{24}\}$ is separable.

In this article, for suboptimal broadcasting, we have considered the inseparability of nonlocal output states $(\tilde{\rho}_{14},\ \tilde{\rho}_{23})$ and separability of local output states on Alice's side $(\tilde{\rho}_{13})$.

2. Broadcasting of quantum discord

In the last decade, it was observed that entanglement is not sufficient to encapsulate all quantum correlations. It was also observed that there are correlations that go beyond the notion of entanglement and these quantum correlations can be used as a resource for some operational tasks as they allow us to do them more efficiently than the conventional classical procedures. It is therefore equally important to broadcast correlations from a pair of states to a larger number of states. In a recent work, we have shown how to broadcast quantum correlations beyond entanglement like quantum discord in $2 \otimes 2$ systems [21,30]. In this article, we have chosen geometric discord (D_G) to quantify the quantum correlations beyond entanglement.

Geometric discord (D_G). The geometric measure of quantum discord D_G is a quantifier of general nonclassical correlations in bipartite quantum states. It is the distance between the quantum state and the nearest classical state. For an arbitrary general qubit-qudit state ρ_{12} (shared by parties numbered 1 and 2), it is defined as $D_G(\rho_{12}) = \min_\chi ||\rho_{12} - \chi||^2$, where χ is the classical state. Such a classical state, in general, can be written as $\chi = \sum_i^{d_1} p_i \pi_i^1 \otimes \rho_i^2$, where d_1 is the dimension of subsystem 1 and π_i^1 are its projectors. ρ_i^2 are density matrices describing states of subsystem 2.

However, for an arbitrary qubit-qudit system, an analytical expression of D_G has been obtained [66], which is defined as follows:

$$D_G(\rho_{12}) = \frac{1}{2d}(||\vec{x}||^2 + ||T||^2 - \lambda_{\max}), \tag{10}$$

where $\vec{x}$ is the Bloch parameter and $\lambda_{\max}$ is the maximal eigenvalue of the matrix $\omega = (\vec{x}\vec{x}^t + TT^t)$. Here superscript "t" denotes the transpose and T is the correlation matrix of ρ_{12}.

Local broadcasting of discord is very similar to the notion of local broadcasting of entanglement. Let D_G be the total amount of discord produced as a result of local cloning operations. D_G^l and D_G^{nl} represent the amount of discord among local and across nonlocal parties, then $D_G = D_G^l + D_G^{nl}$. In order to maximize D_G^{nl}, D_G^l should be ideally zero.

Nonoptimal broadcasting of discord. A quantum correlated state ρ_{12} is said to be broadcast after the application of local cloning operation $(U_a \otimes U_b)$, if the amount of discord of nonlocal output states $\{\tilde{\rho}_{14},\ \tilde{\rho}_{23}\}$ is nonzero for some input state parameters.

Optimal broadcasting of discord. A quantum correlated state ρ_{12} is said to be broadcast optimally after the application of local cloning operation $(U_a \otimes U_b)$, if the amount of discord

of nonlocal output states $\{\tilde{\rho}_{14},\ \tilde{\rho}_{23}\}$ is nonzero and the amount of discord of local output states $\{\tilde{\rho}_{13},\ \tilde{\rho}_{24}\}$ is zero for some input state parameters.

3. Broadcasting of quantum coherence

Quantum coherence has its application in a variety of fields, ranging from quantum information processing to quantum sensing, metrology, thermodynamics [39], and biology [43], and it can act also as a resource in each of these domains. Therefore, it becomes important to investigate the possibility of creating a greater number of coherent states from an existing coherent pair. In a recent study, it has been shown that it is impossible to clone quantum coherence perfectly [67]. In addition to this, just like entanglement, we have shown the possibility of broadcasting coherence using quantum cloning in the $2 \otimes 2$ quantum system [47]. Due to the basis dependent property of quantum coherence, researchers have introduced the concept of genuine quantum coherence which is invariant under change of basis. In the process of cloning we have a blank state (suppose $\rho = \frac{\mathbb{I}}{2}$) which is genuinely an incoherent state. So, if through the process of cloning, we try to increase coherence of the blank state, then the process is termed as broadcasting of quantum coherence. Given a quantum state ρ, the amount of coherence present in the state ρ in the basis $|i\rangle$ is given as follows:

$$C(\rho) = \sum_{i \neq j} |\langle i|\rho|j\rangle|. \tag{11}$$

We will calculate quantum coherence in the two-qubit computational basis $|00\rangle, |01\rangle, |10\rangle, |11\rangle$. This is l_1 norm and it does not depend upon diagonal elements and coherence will be zero in the eigenbasis of the density matrix.

To broadcast coherence between the desired pairs (1,4) and (2,3), one needs to maximize the amount of coherence between the nonlocal output pairs (1,4) and (2,3) irrespective of that between the local output pairs (1,3) and (2,4). In order to broadcast coherence optimally, the amount of coherence between local output pairs should be zero.

Nonoptimal broadcasting of coherence. A coherent input state ρ_{12} is said to be broadcast after the application of local cloning operation $(U_a \otimes U_b)$, if the nonlocal output states $\{\tilde{\rho}_{14}, \tilde{\rho}_{23}\}$ are coherent, i.e., $\mathrm{C}(\tilde{\rho}_{14}) \neq 0, \mathrm{C}(\tilde{\rho}_{23}) \neq 0$ for some input state parameters.

Optimal broadcasting of coherence. A coherent input state ρ_{12} is said to be broadcast optimally after the application of local cloning operation $(U_a \otimes U_b)$, if the nonlocal output states $\{\tilde{\rho}_{14},\ \tilde{\rho}_{23}\}$ are coherent, i.e., $\mathrm{C}(\tilde{\rho}_{14}) \neq 0$ and $\mathrm{C}(\tilde{\rho}_{23}) \neq 0$, while the local output states $\{\tilde{\rho}_{13},\ \tilde{\rho}_{24}\}$ are incoherent, i.e., $\mathrm{C}(\tilde{\rho}_{13}) = 0$ and $\mathrm{C}(\tilde{\rho}_{24}) = 0$, for some input state parameters.

III. BROADCASTING OF ENTANGLEMENT IN $2 \otimes 3$ DIMENSIONS

In this section, we will demonstrate the broadcasting of entanglement in the $2 \otimes 3$ system. Our input resource state is a general qubit-qutrit mixed state ρ_{12} [as in Eq. (2)]. This state is shared between two parties, Alice and Bob. Both of them locally apply the optimal universal symmetric Heisenberg cloning machine as given in Eq. (7).

After cloning, we trace out the ancilla qubit and the ancilla qutrit on Alice's and Bob's side, respectively. The state of this composite system is then given by $\tilde{\rho}_{1234}$. We trace out 2,3 and 1,4 to get the nonlocal output states $\tilde{\rho}_{14}$ and $\tilde{\rho}_{23}$, respectively. Since we are using a symmetric cloner, both the nonlocal output states turn out to be the same.

The expression of the reduced density operator for the nonlocal output states become

$$\tilde{\rho}_{14} = \tilde{\rho}_{23} = \left\{\tfrac{2}{3}\vec{X}, \tfrac{5}{8}\vec{Y}, \tfrac{5}{12}T\right\}. \tag{12}$$

Here $\vec{X} = \{x_i\}_{i\in\{1,2,3\}}$, $\vec{Y} = \{y_j\}_{j\in\{1,\ldots,8\}}$, and T is the correlation matrix of the original input state.

Now, we need to apply the entanglement detection criterion to check the inseparability of nonlocal output states for the case of nonoptimal broadcasting. Since it is not computationally feasible to calculate the eigenvalues of the partial transposed version of the matrix $\tilde{\rho}_{14}$, we cannot apply the Peres-Horodecki criterion in this generalized case to characterize the inseparability region. As a result, we have used the separability criterion [Eq. (6)] in terms of Bloch parameters to check for the separability region of the nonlocal outputs. Since this criterion doesn't satisfy the sufficiency condition, so by applying it we can only comment on the states which are not broadcastable. The nonbroadcastable range is

$$\frac{2}{3}\sum_{j=1}^{8}\sqrt{\sum_{i=1}^{3} t_{ij}^2} \leqslant \frac{12 - 8 * A - 15 * B}{10\sqrt{3}}, \tag{13}$$

where $\mathrm{A} = \sqrt{\sum_{k=1}^{3} x_k^2}$, $\mathrm{B} = \sqrt{\sum_{k=1}^{8} y_k^2}$, and t_{ij} is the element of the i^{th} row and the j^{th} column of the correlation matrix. In other words, for the states which lie beyond the range given in Eq. (13), characterized by this criterion, we cannot say whether they are broadcastable or not broadcastable.

To demonstrate the nonbroadcastable states, we generate 5×10^4 states from a uniform random distribution using the Haar measure. This is displayed in Fig. 2. The states are represented by circles. The states which were successfully characterized to be nonbroadcastable by Eq. (13) are denoted with blue color. On the other hand, the red colored circles denote the states that didn't pass the test in Eq. (13) and so we cannot comment on their usefulness in broadcasting of entanglement. However, they do belong to the class of general mixed states in $2 \otimes 3$ dimensions and are valid density operators. It is important to mention here that the illustration in Fig. 2 is not exhaustive and so doesn't characterize all states in $2 \otimes 3$ dimensions which are not useful for broadcasting. It has only been provided to give a visual perspective of Eq. (13).

To demonstrate the broadcasting of entanglement, we next consider two different classes of mixed entangled states, namely maximally entangled mixed states (Sec. III A) and two-parameter class of states (Sec. III B).

A. Example: maximally entangled mixed states

In this subsection, we consider maximally entangled mixed states as our first example to demonstrate broadcasting of entanglement. MEMS are states with the maximum amount of entanglement for a given degree of mixedness. Its density

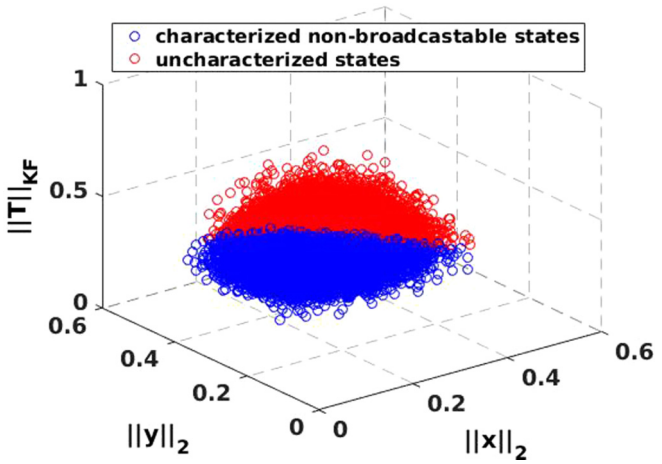

FIG. 2. Blue colored circles denote the states that could be successfully characterized to be not useful for broadcasting of entanglement in $2 \otimes 3$ dimensions out of 5×10^4 states generated uniformly and randomly using the Haar measure. Red colored circles mark the ones out of the 5×10^4 states which didn't pass the separability test in Eq. (13) and so couldn't be characterized either way.

matrix depends on the choice of measures used to quantify entanglement and mixedness. Here, we use linear entropy as a measure for mixedness and square of concurrence as a measure of entanglement. For this choice, the MEMS density matrices are divided into two subclasses (ρ^{MEMSI} and ρ^{MEMSII}) which are defined as follows [68]:

$$\rho^{\text{MEMS}} = \begin{cases} \big(r|\phi^+\rangle\langle\phi^+|, & \\ +\frac{1}{5}\big(1+\frac{r}{2}\big)\big(E_2+E_5\big), & \\ +\frac{1}{5}(1-2r)(E_1+E_3+E_6)\big) & r \in \big[0, \frac{1}{2}\big] \\ r|\phi^+\rangle\langle\phi^+| + \frac{1}{2}(1-r)(E_2+E_5) & r \in \big[\frac{1}{2}, 1\big]. \end{cases} \tag{14}$$

Here, $E_1 = |00\rangle\langle 00|$, $E_2 = |01\rangle\langle 01|$, $E_3 = |02\rangle\langle 02|$, $E_4 = |10\rangle\langle 10|$, $E_5 = |11\rangle\langle 11|$, $E_6 = |12\rangle\langle 12|$, and $|\phi^+\rangle = \frac{1}{\sqrt{2}}(|00\rangle + |12\rangle)$. We denote MEMS density matrix by ρ^{MEMSI} and ρ^{MEMSII} when r ranges from 0 to $\frac{1}{2}$ and $\frac{1}{2}$ to 1, respectively.

1. MEMSI

We apply local optimal cloning transformations [as given in Eq. (7)] for the subclass ρ^{MEMSI}. The expression for the reduced density operator of its nonlocal output states then become

$$\begin{aligned} \tilde{\rho}_{14}^{\text{MEMSI}} &= \big\{\vec{X_{14}}^{\text{MEMSI}}, \vec{Y_{14}}^{\text{MEMSI}}, T_{14}^{\text{MEMSI}}\big\}, \\ \tilde{\rho}_{23}^{\text{MEMSI}} &= \big\{\vec{X_{23}}^{\text{MEMSI}}, \vec{Y_{23}}^{\text{MEMSI}}, T_{23}^{\text{MEMSI}}\big\}, \end{aligned} \tag{15}$$

where $0 \leqslant r \leqslant \frac{1}{2}$, $\vec{X_{14}}^{\text{MEMSI}} = \vec{X_{23}}^{\text{MEMSI}} = \{0, 0, \frac{-2(-1+2r)}{15}\}$, $\vec{Y_{14}}^{\text{MEMSI}} = \vec{Y_{23}}^{\text{MEMSI}} = \{0, 0, \frac{-2-r}{16}, 0, 0, 0, 0, \frac{-2+9r}{16\sqrt{3}}\}$, and the nonzero entries in the correlation matrix ($T_{14}^{\text{MEMSI}} = T_{23}^{\text{MEMSI}}$) are $t_{1,4} = \frac{5r}{12}$, $t_{2,5} = \frac{-5r}{12}$, $t_{3,3} = \frac{2+r}{24}$, and $t_{3,8} = \frac{2+11r}{24\sqrt{3}}$. Here, $t_{i,j}$ denotes the element in the i^{th} row and the j^{th} column of the correlation matrix.

We now apply PH criterion to find out the condition for nonoptimal broadcasting under which the nonlocal output states will be inseparable. We observe that the nonlocal output states are inseparable when the value of r is greater than 0.44.

For optimal broadcasting, we need to check the separability of local output states along with the inseparability of nonlocal output states. The local output states for the input state ρ^{MEMSI} are given by

$$\begin{aligned} \tilde{\rho}_{13}^{\text{MEMSI}} &= \big\{\vec{X_{13}}^{\text{MEMSI}}, \vec{Y_{13}}^{\text{MEMSI}}, T_{13}^{\text{MEMSI}}\big\}, \\ \tilde{\rho}_{24}^{\text{MEMSI}} &= \big\{\vec{X_{24}}^{\text{MEMSI}}, \vec{Y_{24}}^{\text{MEMSI}}, T_{24}^{\text{MEMSI}}\big\}, \end{aligned} \tag{16}$$

where $\vec{X_{13}}^{\text{MEMSI}} = \vec{Y_{13}}^{\text{MEMSI}} = \{0, 0, \frac{2-4r}{15}\}$, $T_{13}^{\text{MEMSI}} = \text{diag}(\frac{1}{3}, \frac{1}{3}, \frac{1}{3})$, $\vec{X_{24}}^{\text{MEMSI}} = \vec{Y_{24}}^{\text{MEMSI}} = \{0, 0, \frac{-2-r}{16}, 0, 0, 0, 0, \frac{-2+9r}{16\sqrt{3}}\}$ and the nonzero entries in the correlation matrix of Bob's side (T_{24}^{MEMSI}) are $t_{1,1} = \frac{6+3r}{40}$, $t_{2,2} = \frac{6+3r}{40}$, $t_{3,3} = \frac{6+3r}{40}$, $t_{4,4} = \frac{3-r}{20}$, $t_{5,5} = \frac{3-r}{20}$, $t_{6,6} = \frac{8-r}{40}$, $t_{7,7} = \frac{8-r}{40}$, $t_{8,8} = \frac{22-9r}{120}$, $t_{3,8} = \frac{-2-r}{40\sqrt{3}}$, and $t_{8,3} = \frac{-2-r}{40\sqrt{3}}$.

Now, for optimal broadcasting, we can apply PH criterion to check the separability of local output states and inseparability of nonlocal output states. Since PH criterion only provides a necessary condition for separability in $3 \otimes 3$ (Bob's side), there can be states that remain positive under partial transposition even if they are entangled. In this case, we therefore can give the suboptimal broadcasting range under which the nonlocal output states are inseparable and the local output state on Alice's side is separable. We observe that the local output states on Alice's side ($2 \otimes 2$) can be always separable irrespective of the value of r. Therefore, the suboptimal broadcasting range is same to the one obtained for nonoptimal broadcasting.

2. MEMSII

We repeat the same procedure for MEMSII where r lies between $\frac{1}{2}$ and 1. Its nonlocal output states are then given by

$$\begin{aligned} \tilde{\rho}_{14}^{\text{MEMSII}} &= \big\{\vec{X_{14}}^{\text{MEMSII}}, \vec{Y_{14}}^{\text{MEMSII}}, T_{14}^{\text{MEMSII}}\big\}, \\ \tilde{\rho}_{23}^{\text{MEMSII}} &= \big\{\vec{X_{23}}^{\text{MEMSII}}, \vec{Y_{23}}^{\text{MEMSII}}, T_{23}^{\text{MEMSII}}\big\}, \end{aligned} \tag{17}$$

where $\vec{X_{14}}^{\text{MEMSII}} = \vec{X_{23}}^{\text{MEMSII}} = \{0, 0, 0\}$, $\vec{Y_{14}}^{\text{MEMSII}} = \vec{Y_{23}}^{\text{MEMSII}} = \{0, 0, \frac{15(-2+3r)}{32}, 0, 0, 0, 0, \frac{-5\sqrt{3}(-2+3r)}{32}\}$ and the nonzero elements in the correlation matrix ($T_{14}^{\text{MEMSII}} = T_{23}^{\text{MEMSII}}$) for nonlocal output states are $t_{1,4} = \frac{5r}{8}$, $t_{2,5} = \frac{-5r}{8}$, $t_{3,3} = \frac{5r}{16}$, and $t_{3,8} = \frac{5\sqrt{3}r}{16}$. Here, $t_{i,j}$ denotes the element in the i^{th} row and the j^{th} column of the correlation matrix.

We again apply PH criterion to find the condition of nonoptimal broadcasting under which the nonlocal output states will be inseparable. We find out that nonlocal output states are always inseparable irrespective of any value of r between $\frac{1}{2}$ and 1. For optimal broadcasting, we check the separability of local output states along with the inseparability of nonlocal output states. The local output states for ρ^{MEMSII} are given by

$$\begin{aligned} \tilde{\rho}_{13}^{\text{MEMSII}} &= \big\{\vec{X_{13}}^{\text{MEMSII}}, \vec{Y_{13}}^{\text{MEMSII}}, T_{13}^{\text{MEMSII}}\big\}, \\ \tilde{\rho}_{24}^{\text{MEMSII}} &= \big\{\vec{X_{24}}^{\text{MEMSII}}, \vec{Y_{24}}^{\text{MEMSII}}, T_{24}^{\text{MEMSII}}\big\}, \end{aligned} \tag{18}$$

where $\vec{X_{13}}^{\text{MEMSII}} = \vec{Y_{13}}^{\text{MEMSII}} = \{0, 0, 0\}$, $T_{13}^{\text{MEMSII}} = \text{diag}(\frac{1}{3}, \frac{1}{3}, \frac{1}{3})$, $\vec{X_{24}}^{\text{MEMSII}} = \vec{Y_{24}}^{\text{MEMSII}} = \{0, 0, \frac{5(-2+3r)}{16}, 0, 0, 0, 0, \frac{5(2-3r)}{16\sqrt{3}}\}$, and the nonzero entries in the correlation matrix of Bob's side (T_{24}^{MEMSII}) are $t_{1,1} = \frac{2-r}{8}, t_{2,2} = \frac{2-r}{8}, t_{3,3} = \frac{2-r}{8}, t_{4,4} = \frac{r}{4}, t_{5,5} = \frac{r}{4}, t_{6,6} = \frac{2-r}{8}, t_{7,7} = \frac{2-r}{8}, t_{8,8} = \frac{(2+3r)}{24}, t_{3,8} = \frac{-2+3r}{8\sqrt{3}}$, and $t_{8,3} = \frac{-2+3r}{8\sqrt{3}}$.

We can apply PH criterion to check the separability of local output states. As stated earlier, there can be states in higher dimension like $3 \otimes 3$ that remains positive under partial transposition even if they are entangled since PH criterion only provides a necessary condition for $3 \otimes 3$ (Bob's side) dimensions. In this case, we therefore can give the suboptimal broadcasting range. We find out that the local output states on Alice's side ($2 \otimes 2$) can be separable when r <0.95. Hence, we conclude that nonoptimal broadcasting is always possible while for suboptimal broadcasting, r should be less than 0.95.

Absolutely separable states. In what follows below, we show that our protocol generates absolutely separable states in Alice's side ($2 \otimes 2$) for some input state parameters. As noted earlier, absolutely separable states preserve their separability under any global unitary operation.

For MEMSI, eigenvalues of Alice's local output state are $\lambda_1 = \frac{6-2r}{15}, \lambda_2 = \frac{1}{3}, \lambda_3 = \frac{4+2r}{15}$, and $\lambda_4 = 0$, such that the condition for absolute separability holds when r is exactly equal to $\frac{1}{2}$.

For MEMSII, eigenvalues of Alice's local output state are $\lambda_1 = \frac{1}{3}, \lambda_2 = \frac{1}{3}, \lambda_3 = \frac{1}{3}$, and $\lambda_4 = 0$, such that the condition for absolute separability holds for every r in range from $\frac{1}{2}$ to 1. Therefore, we can say that absolute separability occurs in the maximally entangled mixed state when r ranges from $\frac{1}{2}$ to 1.

PPT entangled states. As noted earlier in Sec. II D, the realignment criterion is used to detect entanglement in PPT states. By using this criterion, no PPTES on Bob's side ($3 \otimes 3$) were found for any input state parameter in MEMSI. On the other hand, PPTES states on Bob's side ($3 \otimes 3$) were found with MEMSII input states, when r ranges from $\frac{14+4\sqrt{6}}{25}$ to 1. A typical PPTES in this range is given by

$$\begin{bmatrix}
\frac{r}{4} & 0 & 0 & 0 & 0 & 0 & 0 & 0 & 0 \\
0 & \frac{2-r}{16} & 0 & \frac{2-r}{16} & 0 & 0 & 0 & 0 & 0 \\
0 & 0 & \frac{r}{8} & 0 & 0 & 0 & \frac{r}{8} & 0 & 0 \\
0 & \frac{2-r}{16} & 0 & \frac{2-r}{16} & 0 & 0 & 0 & 0 & 0 \\
0 & 0 & 0 & 0 & \frac{1-r}{2} & 0 & 0 & 0 & 0 \\
0 & 0 & 0 & 0 & 0 & \frac{2-r}{16} & 0 & \frac{2-r}{16} & 0 \\
0 & 0 & \frac{r}{8} & 0 & 0 & 0 & \frac{r}{8} & 0 & 0 \\
0 & 0 & 0 & 0 & 0 & \frac{2-r}{16} & 0 & \frac{2-r}{16} & 0 \\
0 & 0 & 0 & 0 & 0 & 0 & 0 & 0 & \frac{r}{4}
\end{bmatrix}.$$

In the next subsection, we demonstrate the broadcasting of entanglement using our second example, a two-parameter class of states.

B. Example: two-parameter class of states

We consider the following class of states with two real parameters α and γ in the $2 \otimes 3$ quantum system [69]:

$$\rho_{\alpha,\gamma} = \alpha(|02\rangle\langle 02| + |12\rangle\langle 12|) + \beta(|\phi^+\rangle\langle\phi^+| + |\phi^-\rangle\langle\phi^-| + |\psi^+\rangle\langle\psi^+|) + \gamma|\phi^-\rangle\langle\psi^-|, \tag{19}$$

where $|\phi^\pm\rangle = \frac{1}{\sqrt{2}}(|00\rangle \pm |11\rangle)$ and $|\psi^\pm\rangle = \frac{1}{\sqrt{2}}(|01\rangle \pm |10\rangle)$ are the four bell states and the parameter β is dependent on α and γ by unit trace condition, $2\alpha + 3\beta + \gamma = 1$. From the unit trace condition, α can vary from 0 to $\frac{1}{2}$ and γ can vary from 0 to 1.

This input state is shared by two parties, Alice and Bob. They both apply local cloning transformations as given by Eq. (7). By tracing out the ancillas and appropriate qubit and qutrit on Alice's and Bob's side, respectively, we get the nonlocal output states which are then given by

$$\tilde{\rho}_{14} = \{\vec{X_{14}}, \vec{Y_{14}}, T_{14}\},$$
$$\tilde{\rho}_{23} = \{\vec{X_{23}}, \vec{Y_{23}}, T_{23}\}, \tag{20}$$

where $\vec{X_{14}} = \vec{X_{23}} = \{0, 0, 0\}$, $\vec{Y_{14}} = \vec{Y_{23}} = \{0, 0, 0, 0, 0, 0, 0, \frac{15-90\alpha}{16\sqrt{3}}\}$, and the nonzero entries in the correlation matrix ($T_{14} = T_{23}$) of nonlocal output states are $t_{1,1} = \frac{5-10\alpha-20\gamma}{24}, t_{2,2} = \frac{5-10\alpha-20\gamma}{24}$, and $t_{3,3} = \frac{5-10\alpha-20\gamma}{24}$. Here, $t_{i,j}$ denotes the element in the i^{th} row and the j^{th} column of the correlation matrix.

Now, we apply the PH criterion to check the inseparability of these nonlocal output states for nonoptimal broadcasting of entanglement. The nonoptimal broadcasting is possible when the following condition is satisfied:

$$\frac{31 - 50\alpha - 40\gamma}{96} < 0. \tag{21}$$

For optimal broadcasting, we also need to check the separability of local output states along with the inseparability of nonlocal output states. The local output states are given by

$$\tilde{\rho}_{13} = \{\vec{X_{13}}, \vec{Y_{13}}, T_{13}\},$$
$$\tilde{\rho}_{24} = \{\vec{X_{24}}, \vec{Y_{24}}, T_{24}\}, \tag{22}$$

where $\vec{X_{13}} = \vec{Y_{13}} = \{0, 0, 0\}$, $T_{13} = \text{diag}(\frac{1}{3}, \frac{1}{3}, \frac{1}{3})$, $\vec{X_{24}} = \vec{Y_{24}} = \{0, 0, 0, 0, 0, 0, 0, \frac{5-30\alpha}{8\sqrt{3}}\}$, and the correlation matrix on Bob's side (T_{24}) is $\text{diag}(\frac{1-2\alpha}{4}, \frac{1-2\alpha}{4}, \frac{1-2\alpha}{4}, \frac{1+2\alpha}{8}, \frac{1+2\alpha}{8}, \frac{1+2\alpha}{8}, \frac{1+2\alpha}{8}, \frac{1+6\alpha}{12})$.

Similar to the case of MEMS, we can only give the suboptimal range as PH criterion is only a necessary condition for $3 \otimes 3$ dimension. The suboptimal broadcasting is only possible when the following inequality is satisfied along with Eq. (21):

$$\frac{3 + 2\alpha - \sqrt{11 - 76\alpha + 204\alpha^2}}{16} \geqslant 0. \tag{23}$$

In Fig. 3, we depict the suboptimal (in dark brown) and nonoptimal (in light yellow) broadcastable regions when the input state is parametrized by α and γ. We observe that the broadcastable region for the suboptimal case is smaller as compared to the nonoptimal one due to the extra separability constraint added on Alice's side in suboptimal broadcasting.

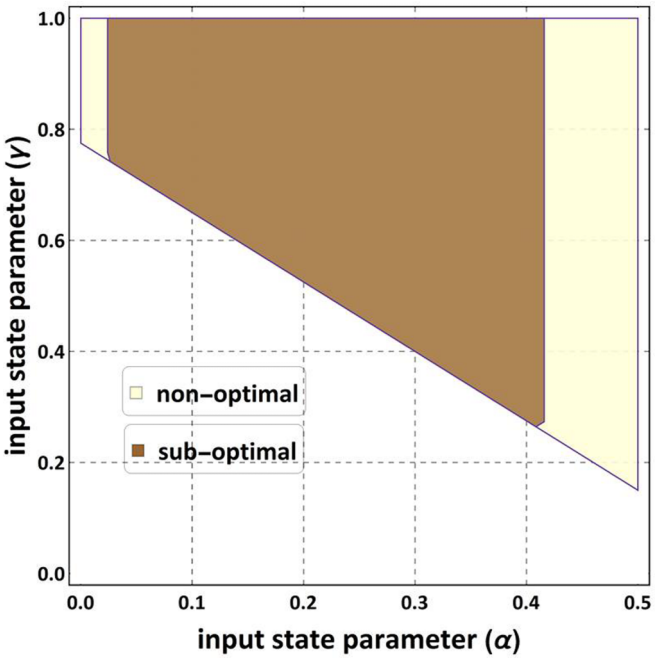

FIG. 3. Plot depicting the suboptimal (in dark brown) as well as nonoptimal (in light yellow) broadcastable region for the input TPCS in terms of two input state parameters: α and γ.

Absolutely separable states. Like maximally entangled mixed states, our protocol generates absolutely separable states on Alice's side $(2 \otimes 2)$ with input TPCS, too. The eigenvalues of the local output state on Alice's side are $\lambda_1 = \frac{1}{3}, \lambda_2 = \frac{1}{3}, \lambda_3 = \frac{1}{3}$, and $\lambda_4 = 0$, so the absolute separability condition holds over the entire range of input state parameters.

PPT entangled states. Similar to MEMSII, our protocol generates PPTES on Bob's side $(3 \otimes 3)$ also with input TPCS. PPTES are found at the output when state parameter α ranges from 0 to $\frac{11-4\sqrt{6}}{50}$ and $\frac{11+4\sqrt{6}}{50}$ to $\frac{1}{2}$. A typical PPTES in this range is given by

$$\begin{bmatrix}
\frac{1-2\alpha}{4} & 0 & 0 & 0 & 0 & 0 & 0 & 0 & 0 \\
0 & \frac{1-2\alpha}{8} & 0 & \frac{1-2\alpha}{8} & 0 & 0 & 0 & 0 & 0 \\
0 & 0 & \frac{1+2\alpha}{16} & 0 & 0 & 0 & \frac{1+2\alpha}{16} & 0 & 0 \\
0 & \frac{1-2\alpha}{8} & 0 & \frac{1-2\alpha}{8} & 0 & 0 & 0 & 0 & 0 \\
0 & 0 & 0 & 0 & \frac{1-2\alpha}{4} & 0 & 0 & 0 & 0 \\
0 & 0 & 0 & 0 & 0 & \frac{1+2\alpha}{16} & 0 & \frac{1+2\alpha}{16} & 0 \\
0 & 0 & \frac{1+2\alpha}{16} & 0 & 0 & 0 & \frac{1+2\alpha}{16} & 0 & 0 \\
0 & 0 & 0 & 0 & 0 & \frac{1+2\alpha}{16} & 0 & \frac{1+2\alpha}{16} & 0 \\
0 & 0 & 0 & 0 & 0 & 0 & 0 & 0 & \alpha
\end{bmatrix}.$$

IV. BROADCASTING OF DISCORD AND COHERENCE IN $2 \otimes d$ DIMENSIONS

As discussed before, entanglement is not the only resource. There are correlations that go beyond entanglement: quantum discord. Other than quantum correlations that go beyond entanglement (quantum discord), quantum coherence (l_1 norm) is also extensively used as a resource. Hence, a resource theory framework is created for describing them [36]. In this section, we consider broadcasting of these resources in the qubit-qudit system, where one of the parties says Alice is having a two-level system whereas the other party in general is having a d-level system. The goal is again to create a greater number of resource states through broadcasting using the optimal universal symmetric Heisenberg cloning machine. In this process, we find out that it is impossible to broadcast these resources optimally in a qubit-qudit system. However, nonoptimal broadcasting can still be done and we exemplify such cases of broadcasting in this section.

A. Optimal broadcasting of discord and coherence

In this subsection, we show that optimal broadcasting of quantum discord and quantum coherence is not possible in the $(2 \otimes d)$-dimensional system.

Theorem 1. Given a general bipartite mixed quantum state in $2 \otimes d$ dimension ρ_{12} [Eq. (1)] and Heisenberg local cloning transformations [Eq. (7)], it is impossible to broadcast the quantum discord [D_G as defined in Eq. (10)] within ρ_{12} optimally into two lesser quantum correlated states: $\{\tilde{\rho}_{14}, \tilde{\rho}_{23}\}$.

Proof: Let us assume that the two parties Alice and Bob share a general qubit-qudit quantum mixed state ρ_{12}. We then apply local Heisenberg optimal cloning transformations (7) to qubits "1" and "3" and qudit "2" and "4" on Alice's side and Bob's side, respectively; "5" and "6" are the machine states on Alice's side and Bob's side, respectively. By tracing out the machine states and Bob's side qudits, we get the local output state on Alice's part as $\tilde{\rho}_{13} = \{\frac{2}{3}\vec{x}, \frac{2}{3}\vec{x}, T^{13}\}$, where $T^{13} = \text{diag}(\frac{1}{3}, \frac{1}{3}, \frac{1}{3})$ and $\vec{x} = \{x_i\}_{i\in\{1,2,3\}}$. We observe that the local output state on Alice's side does not depend on the dimension d of Bob's side (see Appendix). The geometric discord D_G calculated using Eq. (10) of the local output state comes out to be constant, i.e., $D_G(\tilde{\rho}_{13}) = \frac{1}{18}$ which always remains nonzero. For optimal broadcasting, we need the $D_G(\tilde{\rho}_{13})$ and $D_G(\tilde{\rho}_{24})$ both to be zero. Hence optimal broadcasting of quantum discord is not possible in the case of the qubit-qudit system as $D_G(\tilde{\rho}_{13}) \neq 0$.

Theorem 2. Given a general qubit-qudit mixed quantum state ρ_{12} and Heisenberg optimal cloning transformations, it is impossible to broadcast the quantum coherence optimally within ρ_{12} into two coherent states: $\{\tilde{\rho}_{14}, \tilde{\rho}_{23}\}$.

Proof. We consider the input state shared between Alice and Bob as the most general qubit-qudit state ρ_{12}. We apply Heisenberg local cloning transformation $U_a \otimes U_b$ to clone the qubit $1 \to 3$ and qudit $2 \to 4$ on Alice's side and Bob's side, respectively. By tracing out the machine states and Bob's side qudits, we get the local output state on Alice's part as $\tilde{\rho}_{13} = \{\frac{2}{3}\vec{x}, \frac{2}{3}\vec{x}, T^{13}\}$, where $T^{13} = \text{diag}(\frac{1}{3}, \frac{1}{3}, \frac{1}{3})$ and $\vec{x} = \{x_i\}_{i\in\{1,2,3\}}$. The coherence given by the l_1 norm [Eq. (11)] of the local output state on Alice's side comes out to be $C(\tilde{\rho}_{13}) = \frac{1}{3} + (\frac{4}{3})\sqrt{x_1^2 + x_2^2} > 0$. For optimal broadcasting, we need $C(\tilde{\rho}_{13})$ and $C(\tilde{\rho}_{24})$ both to be zero. Hence, it is evident that it is impossible to broadcast coherence optimally.

B. Nonoptimal broadcasting of discord and coherence for MEMS and TPCS states

In the previous subsection, we have seen that optimal broadcasting of quantum discord (D_G) and coherence (l_1 norm) is not possible for $2 \otimes d$ systems via optimal universal

TABLE II. This table gives the range for nonoptimal broadcasting of geometric discord (D_G) for the MEMS class of states.

States	$D_G(\tilde{\rho}_{14})$	$D_G(\tilde{\rho}_{13})$	Range
MEMSI	$\frac{25r^2}{192}$	$\frac{1}{18}$	$r > 0$
MEMSII	$\frac{25r^2}{192}$	$\frac{1}{18}$	$r > 0$

Heisenberg local cloning operations. However, this never rules out the possibility of nonoptimal broadcasting of these resources by using the same cloner. In this subsection we take the same qubit-qutrit examples: (a) maximally entangled mixed states and (b) two-parameter class of states. We show that nonoptimal broadcasting is indeed possible to a certain range of input state parameters. In particular, we find out the range based on the input state parameters for which such broadcasting will be possible.

1. MEMS

We apply local cloning transformation [Eq. (7)] to MEMSI and MEMSII separately. We trace out the machine states and the respective qubits and qutrits to get the nonlocal output states($\tilde{\rho}_{14}$, $\tilde{\rho}_{23}$). Then, we calculate the geometric discord [Eq. (10)] of nonlocal output states. For nonoptimal broadcasting, $D_G(\tilde{\rho}_{14})$ and $D_G(\tilde{\rho}_{23})$ is nonzero for some input state parameter. In Table II, we give the range for nonoptimal broadcasting of geometric discord for the subclasses: MEMSI and MEMSII.

For nonoptimal broadcasting of coherence, we calculate the l_1 norm [Eq. (11)] of nonlocal output states. Again for nonoptimal broadcasting, $C(\tilde{\rho}_{14})$ and $C(\tilde{\rho}_{23})$ are nonzero for some input state parameters. In Table III, we give the range for non-optimal broadcasting of coherence for the subclasses: MEMSI and MEMSII.

2. TPCS

We repeat the same procedure as above for the two-parameter class of states to find the range for nonoptimal broadcasting of geometric discord [Eq. (10)] in terms of input state parameters (α and γ). The expression for geometric discord comes out to be

$$D_G(\tilde{\rho}_{14}) = \frac{25(-1+2\alpha+4\gamma)^2}{288}. \tag{24}$$

We can clearly see that nonoptimal broadcasting is possible for the entire range of α and γ except for the points when $\alpha = \frac{1-4\gamma}{2}$.

Though it is impossible to broadcast quantum coherence optimally but we can broadcast it nonoptimally. We find the range for nonoptimal broadcasting of coherence [Eq. (11)] in terms of input state parameters (α and γ). The expression for coherence (l_1 norm) comes out to be

$$C(\tilde{\rho}_{14}) = \left|\frac{5-10\alpha-20\gamma}{36}\right|. \tag{25}$$

We can clearly observe that nonoptimal broadcasting is possible for the entire range of α and γ except for the points when $\alpha = \frac{1-4\gamma}{2}$. The broadcasting range for both discord and coherence with respect to input state parameters α and γ is shown in Fig. 4 and Fig. 5, respectively.

TABLE III. This table gives the range for nonoptimal broadcasting of coherence (l_1 norm) for the MEMS class of states.

States	$C(\tilde{\rho}_{14})$	$C(\tilde{\rho}_{13})$	Range
MEMSI	$\frac{5r}{12}$	$\frac{1}{3}$	$r > 0$
MEMSII	$\frac{5r}{12}$	$\frac{1}{3}$	$r > 0$

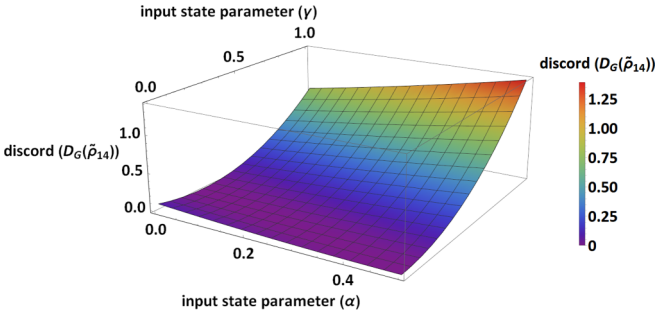

FIG. 4. The 3D plot shows the variation of geometric discord (D_G) of the nonlocal output state $\tilde{\rho}_{14}$ as a function of input state parameters α and γ for the two-parameter class of states.

V. CONCLUSION

The present work deals with the broadcasting of quantum resources beyond qubit-qubit systems. In particular, we investigate the problem of broadcasting of entanglement for a general qubit-qutrit ($2 \otimes 3$) state and are able to identify the set of states for which the broadcasting will never be possible. We take examples like (a) maximally entangled mixed states and (b) two-parameter class of states from $2 \otimes 3$ systems to show the range of both suboptimal and nonoptimal broadcasting. We show that it is impossible to optimally broadcast quantum discord and quantum coherence optimally for general $2 \otimes d$-dimensional systems. Furthermore, to show that the nonoptimal broadcasting of these resources is still a possibility, we consider the same examples from $2 \otimes 3$ systems and thereafter find out the range of the input state parameters for which it will be possible.

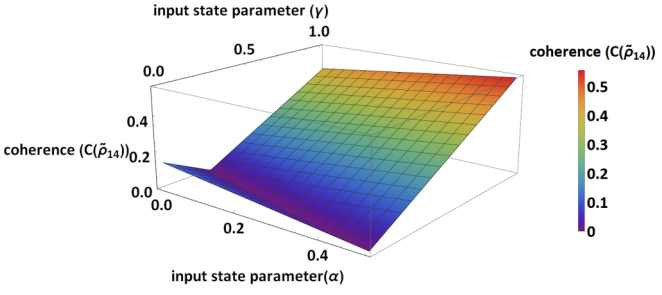

FIG. 5. The 3D plot shows the variation of coherence (l_1 norm) of nonlocal output state $\tilde{\rho}_{14}$ as a function of input state parameters α and γ for the two-parameter class of states.

Our protocol in $2 \otimes 3$ dimensions also results in states on the qubit side which are absolutely separable in two-qubit systems. Generation of entangled states on the qutrit side having a positive partial transpose purely from physical consideration is another significant derivative of the work presented here. However, our work focuses on broadcasting of quantum resources in the qubit-qutrit and qubit-qudit scenarios. This work calls attention to an extension of arbitrary dimensions in bipartite and multipartite systems.

ACKNOWLEDGMENTS

N.G. would like to acknowledge support from the Research Initiation Grant of BITS-Pilani, Hyderabad (Letter No. BITS/GAU/RIG/2019/H0680 dated April 22, 2019). S.C. acknowledges the internship grant from Erlangen Graduate School in Advanced Optical Technologies (SAOT) for supporting the research work as an intern at IIIT, Hyderabad, and HRI, Allahabad in India.

APPENDIX

Consider the two parties Alice and Bob share a general mixed state in $2 \otimes d$ dimension (ρ_{12}) as defined in Eq. (1). Both parties apply a local optimal symmetric Heisenberg cloner on their respective sides. The blank state on Alice's and Bob's side is represented with suffixes "3" and "4" respectively. The initial state of the cloners on Alice's side and Bob's side is denoted by "5" and "6" respectively. The state of the composite system can be represented by ρ_{123456}. U_a and U_b are the cloning operators on Alice's side and Bob's side, respectively. We then trace out "2", "4", "6" subsystems from Bob's side, after the application of the cloning machine, to get

$$
\begin{aligned}
\rho_{135} &= \mathrm{Tr}_{246}[(U_a \otimes U_b)\rho_{123456}(U_a' \otimes U_b')] \\
&= \mathrm{Tr}_{246}\left[(U_a \otimes U_b)\frac{1}{2d}\left(\mathbb{I}_2 \otimes \mathbb{I}_d + \sum_{i=1}^{3} x_i\sigma_i \otimes \mathbb{I}_d + \sum_{i=1}^{d^2-1} y_i \mathbb{I}_2 \otimes O_i + \sum_{i=1}^{3}\sum_{j=1}^{d^2-1} t_{ij}\sigma_i \otimes O_j\right) \otimes \rho_{35} \otimes \rho_{46}(U_a' \otimes U_b')\right] \\
&= \mathrm{Tr}_{246}\left[(U_a \otimes U_b)\frac{1}{2d}\left(\mathbb{I}_2 \otimes \mathbb{I}_d \otimes \rho_{35} \otimes \rho_{46} + \sum_{i=1}^{3} x_i\sigma_i \otimes \mathbb{I}_d \otimes \rho_{35} \otimes \rho_{46} + \sum_{i=1}^{d^2-1} y_i \mathbb{I}_2 \otimes O_i \otimes \rho_{35} \otimes \rho_{46}\right.\right. \\
&\quad \left.\left. + \sum_{i=1}^{3}\sum_{j=1}^{d^2-1} t_{ij}\sigma_i \otimes O_j \otimes \rho_{35} \otimes \rho_{46}\right)(U_a' \otimes U_b')\right] \\
&= \mathrm{Tr}_{246}\left[\frac{1}{2d}\left(U_a(\mathbb{I}_2 \otimes \rho_{35})U_a' \otimes U_b(\mathbb{I}_d \otimes \rho_{46})U_b' + \sum_{i=1}^{3} x_i U_a(\sigma_i \otimes \rho_{35})U_a' \otimes U_b(\mathbb{I}_d \otimes \rho_{46})U_b'\right.\right. \\
&\quad \left.\left. + \sum_{i=1}^{d^2-1} y_i U_a(\mathbb{I}_2 \otimes \rho_{35})U_a' \otimes U_b(O_i \otimes \rho_{46})U_b' + \sum_{i=1}^{3}\sum_{j=1}^{d^2-1} t_{ij} U_a(\sigma_i \otimes \rho_{35})U_a' \otimes U_b(O_j \otimes \rho_{46})U_b'\right)\right] \\
&= \frac{1}{2d}[\mathrm{Tr}_{246}[U_a(\mathbb{I}_2 \otimes \rho_{35})U_a' \otimes U_b(\mathbb{I}_d \otimes \rho_{46})U_b']] + \frac{1}{2d}\left[\mathrm{Tr}_{246}\left[\sum_{i=1}^{3} x_i U_a(\sigma_i \otimes \rho_{35})U_a' \otimes U_b(\mathbb{I}_d \otimes \rho_{46})U_b'\right]\right] \\
&\quad + \frac{1}{2d}\left[\mathrm{Tr}_{246}\left[\sum_{i=1}^{d^2-1} y_i U_a(\mathbb{I}_2 \otimes \rho_{35})U_a' \otimes U_b(O_i \otimes \rho_{46})U_b'\right]\right] + \frac{1}{2d}\left[\mathrm{Tr}_{246}\left[\sum_{i=1}^{3}\sum_{j=1}^{d^2-1} t_{ij} U_a(\sigma_i \otimes \rho_{35})U_a' \otimes U_b(O_j \otimes \rho_{46})U_b'\right]\right].
\end{aligned}
\tag{A1}
$$

The reduced density matrix on Alice's side is given by $\rho_{135} = \frac{1}{2}[U_a(\mathbb{I}_2 \otimes \rho_{35})U_a' + \sum_{i=1}^{3} x_i U_a(\sigma_i \otimes \rho_{35})U_a']$ as unitary transformation doesn't affect the inner product of the system. Also, σ_i's and O_j's are traceless matrices and are independent of the dimension of Bob's side. Therefore, on application of the cloning transformations given by Eq. (7) on a general bipartite mixed state in $2 \otimes d$ dimension [Eq. (1)], the marginal state of Alice remains independent of the dimension "d" of Bob's side.

[1] R. Horodecki, P. Horodecki, M. Horodecki, and K. Horodecki, Rev. Mod. Phys. **81**, 865 (2009).

[2] R. Bedington, J. M. Arrazola, and A. Ling, npj Quant. Inf. **3**, 30 (2017).

[3] C. H. Bennett, G. Brassard, C. Crépeau, R. Jozsa, A. Peres, and W. K. Wootters, Phys. Rev. Lett. **70**, 1895 (1993); R. Horodecki, M. Horodecki, and P. Horodecki, Phys. Lett. A **222**, 21 (1996).

[4] C. H. Bennett and S. J. Wiesner, Phys. Rev. Lett. **69**, 2881 (1992); R. Nepal, R. Prabhu, A. Sen(De), and U. Sen, Phys. Rev. A **87**, 032336 (2013).

[5] M. Hillery, V. Buzek, and A. Berthiaume, Phys. Rev. A **59**, 1829 (1999); S. Sazim *et al.*, Quantum. Inf. Process. **14**, 4651 (2015); S. Adhikari, I. Chakrabarty, and P. Agrawal, Quant. Inf. Comp. **12**, 253 (2012); M. Ray, S. Chatterjee, and I. Chakrabarty, Eur. Phys. J. D **70**, 114 (2016).

[6] A. K. Ekert, Phys. Rev. Lett. **67**, 661 (1991).

[7] D. Gottesman and I. Chuang, arXiv:quant-ph/0105032; C. Croal, C. Peuntinger, B. Heim, I. Khan, C. Marquardt, G. Leuchs, P. Wallden, E. Andersson, and N. Korolkova, Phys. Rev. Lett. **117**, 100503 (2016).

[8] S. Sazim and I. Chakrabarty, Eur. Phys. J. D **67**, 174 (2013).

[9] C. A. Sackett *et al.*, Nature (London) **404**, 256 (2000); A. Rauschenbeutel *et al.*, Science **288**, 2024 (2000); B. Kraus and J. I. Cirac, Phys. Rev. A **63**, 062309 (2001); B. P. Lanyon and N. K. Langford, New J. Phys. **11**, 013008 (2009); M. J. Kastoryano, F. Reiter, and A. S. Sorensen, Phys. Rev. Lett. **106**, 090502 (2011).

[10] S. L. Braunstein, C. M. Caves, R. Jozsa, N. Linden, S. Popescu, and R. Schack, Phys. Rev. Lett. **83**, 1054 (1999); D. O. Soares-Pinto *et al.*, Philos. Trans. R. Soc. London A **370**, 4821 (2012).

[11] M. Horodecki, P. Horodecki, and R. Horodecki, Phys. Rev. Lett. **80**, 5239 (1998).

[12] P. Horodecki, Phys. Lett. A **232**, 333 (1997).

[13] M. Ozols, G. Smith, and J. A. Smolin, Phys. Rev. Lett. **112**, 110502 (2014).

[14] H. J. Kimble, Nature (London) **453**, 1023 (2008).

[15] S. Wehner, D. Elkouss, and R. Hanson, Science **362**, eaam9288 (2018).

[16] M. Pant *et al.*, npj Quant. Inf. **5**, 25 (2019).

[17] J. I. Cirac, A. Ekert, S. F. Huelga, and C. Macchiavello, Phys. Rev. A **59**, 4249 (1999).

[18] D. Gottesman, T. Jennewein, and S. Croke, Phys. Rev. Lett. **109**, 070503 (2012).

[19] A. Broadbent, J. Fitzsimons, and E. Kashefi, in *2009 50th Annual IEEE Symposium on Foundations of Computer Science* (IEEE, Atlanta, 2009), pp. 517–526.

[20] V. Buzek, V. Vedral, M. B. Plenio, P. L. Knight, and M. Hillery, Phys. Rev. A **55**, 3327 (1997).

[21] S. Chatterjee, S. Sazim, and I. Chakrabarty, Phys. Rev. A **93**, 042309 (2016).

[22] V. Buzek and M. Hillery, Phys. Rev. Lett. **81**, 5003 (1998).

[23] W. K. Wootters and W. H. Zurek, Nature (London) **299**, 802 (1982).

[24] S. Luo, Lett. Math. Phys. **92**, 143 (2010); S. Luo, N. Li, and X. Cao, Phys. Rev. A **79**, 054305 (2009); M. Piani, P. Horodecki, and R. Horodecki, Phys. Rev. Lett. **100**, 090502 (2008).

[25] V. Buzek and M. Hillery, Phys. Rev. A **54**, 1844 (1996).

[26] N. Gisin and S. Massar, Phys. Rev. Lett. **79**, 2153 (1997).

[27] S. Bandyopadhyay and G. Kar, Phys. Rev. A **60**, 3296 (1999).

[28] N. Gisin, Phys. Lett. A **242**, 1 (1998).

[29] I. Ghiu, Phys. Rev. A **67**, 012323 (2003).

[30] A. Jain, I. Chakrabarty, and S. Chatterjee, Phys. Rev. A **99**, 022315 (2019).

[31] H. Ollivier and W. H. Zurek, Phys. Rev. Lett. **88**, 017901 (2001).

[32] L. Henderson and V. Vedral, J. Phys. A **34**, 6899 (2001).

[33] S. Adhikari and S. Banerjee, Phys. Rev. A **86**, 062313 (2012).

[34] A. L. Malvezzi, G. Karpat, B. Çakmak, F. F. Fanchini, T. Debarba, and R. O. Vianna, Phys. Rev. B **93**, 184428 (2016).

[35] B. Dakic *et al.*, Nature Physics **8**, 666 (2012).

[36] A. Winter and D. Yang, Phys. Rev. Lett. **116**, 120404 (2016).

[37] T. Baumgratz, M. Cramer, and M. B. Plenio, Phys. Rev. Lett. **113**, 140401 (2014).

[38] J. B. Brask and N. Brunner, Phys. Rev. E **92**, 062101 (2015).

[39] M. Lostaglio, D. Jennings, and T. Rudolph, Nat. Commun. **6**, 6383 (2015).

[40] N. Anand and A. K. Pati, arXiv:1611.4542.

[41] H.-L. Shi, S.-Y. Liu, X.-H. Wang, W.-L. Yang, Z.-Y. Yang, and H. Fan, Phys. Rev. A **95**, 032307 (2017).

[42] A. Olaya-Castro, C. F. Lee, F. F. Olsen, and N. F. Johnson, Phys. Rev. B **78**, 085115 (2008).

[43] J. N. Bandyopadhyay, T. Paterek, and D. Kaszlikowski, Phys. Rev. Lett. **109**, 110502 (2012).

[44] M. N. Bera, T. Qureshi, M. A. Siddiqui, and A. K. Pati, Phys. Rev. A **92**, 012118 (2015).

[45] Y. Yuan *et al.*, Opt. Express **26**, 4470 (2018).

[46] D. Abbott, P. C. W. Davies, and A. K. Pati, *Quantum Aspects of Life* (Imperial College Press, London, 2008).

[47] U. K. Sharma, I. Chakrabarty, and M. K. Shukla, Phys. Rev. A **96**, 052319 (2017).

[48] I. Marvian and R. W. Spekkens, Phys. Rev. A **94**, 052324 (2016).

[49] J. I. de Vicente and A. Streltsov, J. Phys. A **50**, 045301 (2017); A. Streltsov, G. Adesso, and M. B. Plenio, Rev. Mod. Phys. **89**, 041003 (2017); A. Streltsov, S. Rana, P. Boes, and J. Eisert, Phys. Rev. Lett. **119**, 140402 (2017).

[50] M. Lostaglio and M. P. Müller, Phys. Rev. Lett. **123**, 020403 (2019); I. Marvian and R. W. Spekkens, *ibid.* **123**, 020404 (2019).

[51] M. Erhard *et al.*, Light: Sci. Appl. **7**, 17146 (2018).

[52] D. Kaszlikowski, P. Gnaciński, M. Żukowski, W. Miklaszewski, and A. Zeilinger, Phys. Rev. Lett. **85**, 4418 (2000).

[53] M. Huber and M. Pawlowski, Phys. Rev. A **88**, 032309 (2013).

[54] E. T. Campbell, H. Anwar, and D. E. Browne, Phys. Rev. X **2**, 041021 (2012).

[55] A. Bocharov, M. Roetteler, and K. M. Svore, Phys. Rev. A **96**, 012306 (2017).

[56] N. J. Cerf, M. Bourennane, A. Karlsson, and N. Gisin, Phys. Rev. Lett. **88**, 127902 (2002).

[57] H. Bechmann-Pasquinucci and W. Tittel, Phys. Rev. A **61**, 062308 (2000).

[58] V. Coffman, J. Kundu, and W. K. Wootters, Phys. Rev. A **61**, 052306 (2000).

[59] M. Horodecki, P. Horodecki, and R. Horodecki, Phys. Lett. A **223**, 1 (1996).

[60] J. I. D. Vicente, Quantum Inf. Comput. **7**, 624 (2007).

[61] M. Kus and K. Zyczkowski, Phys. Rev. A **63**, 032307 (2001).

[62] F. Verstraete, K. Audenaert, and B. DeMoor, Phys. Rev. A **64**, 012316 (2001).

[63] N. Johnston, Phys. Rev. A **88**, 062330 (2013).
[64] N. Ganguly, J. Chatterjee, and A. S. Majumdar, Phys. Rev. A **89**, 052304 (2014).
[65] E. W. Weisstein, MathWorld, http://mathworld.wolfram.com, retrieved April, 12, 2017.
[66] S. Vinjanampathy and A. R. P. Rau, J. Phys. A **45**, 095303 (2012).
[67] D. Patel *et al.*, arXiv:1806.5706.
[68] S. R. Hedemann, arXiv:1310.7038.
[69] D. P. Chi and S. Lee, J. Phys. A **36**, 11503 (2003).